

PTP61F Mediates Cell Competition

Subjects: Cell Biology

Submitted by:  Helena Richardson

Definition

Tissue homeostasis via the elimination of aberrant cells is fundamental for organism survival. Cell competition is a key homeostatic mechanism, contributing to the recognition and elimination of aberrant cells, preventing their malignant progression and the development of tumors.

1. Introduction

The vinegar fly, *Drosophila melanogaster*, is a valuable organism for modelling many human disorders, including cancer. Most of the “hallmarks of cancer” are able to be modelled in *Drosophila*, and along with the conservation ~70% of disease-relevant genes and its short life cycle, makes *Drosophila* a useful model for studying tumorigenesis (reviewed in ^{[1][2][3]}). Indeed *Drosophila* is a useful model organism for studying cooperative tumorigenesis—such as upon the activation of the GTPase RAS85D (commonly referred to as RAS, human orthologues HRAS/KRAS/NRAS) and loss of the apico-basal cell polarity regulators Scribble (SCRIB) or Discs large 1 (DLG1) (human orthologues SCRIB and DLG1-4, respectively) (reviewed in ^[4]). These alterations cooperate to promote the formation of neoplastic, invasive tumors in developing *Drosophila* larvae via the the promotion of cell proliferation and anti-apoptotic signals, and contribute to the co-option of c-Jun N-terminal Kinase (JNK) signalling into a proliferation-promoting signalling pathway (reviewed in ^[5]). However, individually activating RAS85D or impairing polarity cause only “pre-tumorigenic” tissue disruptions—RAS85D activation ^{[6][7]}, while polarity impairment leads to increased cell proliferation but also cell death, differentiation defects, and increased cell migration/invasion ^{[7][8][9][10][11][12][13][14]}. When entire tissues are depleted of SCRIB or DLG1 massive overgrowth occurs, but when *scrib* or *dlg1* mutant cells are generated in a clonal manner in *Drosophila* developing epithelial tissues (the wing or eye-antennal imaginal discs), these cells are subject to a tissue surveillance and homeostasis mechanism known as cell competition ^{[10][15]}. The core concept of cell competition is that the fitness of each cell is surveyed relative to their neighbouring cells, and cells that are less fit are actively eliminated to maintain tissue homeostasis (reviewed in ^[16]). This is an evolutionarily conserved mechanism, though it is less studied in mammals compared with flies (reviewed in ^[17]). The eliminated cells are termed “loser cells”, while those that eliminate and replace them are termed “winner cells”. In *Drosophila* epithelial tissues, *scrib/dlg1* mutant clones undergo cell competition, and are eliminated by their *wild-type* neighbours ^{[10][15]}. Mechanistically, the modulation of several signalling pathways is required for the elimination of polarity-impaired cells during cell competition, including the JNK, the Hippo tissue growth inhibitory, the Janus kinase-signal transducer and activator of transcription (JAK-STAT), and the Epidermal Growth Factor Receptor (EGFR)-RAS-Mitogen Activated Protein Kinase (MAPK) signalling pathways (reviewed in ^[16]). The precise functions and targets of each cell competition-induced signalling pathway and the interplay between them are not completely understood, but many involve protein tyrosine kinase (PTK) pathways, and therefore the investigation in cell competition of protein tyrosine phosphatases (PTPs) that regulate these pathways is a logical step.

The spatial and temporal activity of many signalling pathways are regulated by phosphorylation of proteins by protein kinases and dephosphorylation by protein phosphatases. Protein phosphatases are classified into three groups: protein serine/threonine phosphatases, PTPs, and dual-specificity phosphatases (DUSPs) (reviewed in ^{[18][19][20]}). Serine/threonine phosphorylation is the major type of protein phosphorylation in mammalian cells, but tyrosine phosphorylation-dependent signalling is critical for the relaying of cues from the extracellular environment and for cell-cell communication. More than 100 structurally and functionally diverse PTPs have been identified in the human genome ^[20], whilst in *Drosophila melanogaster*, there are currently 44 known PTPs (including DUSPs), all with conserved human orthologues, though not all human PTPs have fly orthologues ^{[21][22][23]}. PTPs in *Drosophila*, as in

mammals, belong to either the transmembrane receptor or non-receptor subtypes [21]. The *Drosophila* non-receptor protein tyrosine phosphatase 61F (Ptp61F) functions as a negative regulator in a number of highly conserved signalling pathways, including the JAK-STAT pathway [24][25][26][27], the Insulin-like Receptor (INR) pathway [24][27][28][29], the EGFR pathway [27][28], and the Platelet-Derived Growth Factor (PDGF)- and Vascular Endothelial Growth Factor (VEGF)-receptor-related (PVR) pathway [27]. The mammalian orthologs of PTP61F are PTP1B (encoded by PTPN1) and TCPTP (encoded by PTPN2), which share 74% catalytic domain sequence identity and 86% similarity, respectively (reviewed in [30][31]). PTP1B, the first mammalian PTP identified [32], is localised to the cytoplasmic face of the endoplasmic reticulum and plays an important role in immunity and metabolism, acting to dephosphorylate substrates such as the INR [33][34][35] and JAK-family PTKs JAK-2 and Tyk2 [36]. PTP1B can act as a tumor suppressor, but also has oncogenic roles as the upregulation of PTP1B can contribute to the activation of SRC-family PTKs [37][38] and mediate signalling by the HER-2 oncoprotein [39][40]. PTPN2 encodes two splice variants: A 48 kDa TCPTP (TC48) which, like PTP1B, is localised to the endoplasmic reticulum, and a 45 kDa variant (TC45) that is targeted to the nucleus but shuttles between the nuclear and cytoplasmic environments [41][42][43][44]. Thus, TCPTP has access to both nuclear substrates, such as STAT-1/3/5, and cytoplasmic substrates, such as INR and JAK-1/3 [31][44]. TCPTP and PTP1B have both overlapping and distinct functions in mammals [31]. TCPTP is thought to serve as a tumor suppressor, particularly in T cell acute lymphoblastic leukemia [45][46], but also there is evidence in breast cancer [47] and liver cancer [48][49]. However, the role of Ptp61F in *Drosophila* cancer models has not been explored.

2. Ptp61F Impairment Confers a Competitive Advantage on Epithelial Clones

Various highly conserved well-characterised signalling pathways, such as EGFR-RAS-MAPK and JAK-STAT signalling, are involved in cell competition in *Drosophila* epithelial tissues (reviewed in [16]). Since the regulation of these pathways are orchestrated by reversible tyrosine phosphorylation, the authors reasoned that PTPs might play an unappreciated role in cell competition. The *Drosophila* tyrosine phosphatase protein tyrosine phosphatase 61F (Ptp61F) was selected as a candidate to investigate, as it has been shown to negatively regulate EGFR-RAS-MAPK and JAK-STAT signalling [27].

First, the authors utilised a technique known as “twin-clone generation”, whereby a single recombination event simultaneously generates GFP-double-positive *wild-type* clones and GFP-negative mutant clones, in a background of GFP-single-positive *wild-type* *Drosophila* third-instar larval (L3) epithelial tissues (technique adapted from Froidi et al. [50]). In control third instar larval (L3) wing imaginal discs, the generation of twin-clones where both are *wild-type*, although one twin is GFP-double positive and the other is GFP negative (**Figure 1A,A'**), leads to clones where the GFP-double-positive clones are consistently slightly larger than their GFP-negative twins, perhaps due to background genetic effects (**Figure 1E**). However, when the GFP-negative clones are homozygous mutant for *Ptp61F* (**Figure 1B,B'**), using the null allele *Ptp61F^Δ* [24], the trend was reversed and *Ptp61F^{Δ/Δ}* clones are consistently larger than their *wild-type* twins (**Figure 1E**). Analysing the GFP-negative/GFP-double-positive size ratio for each twin-clone pair further revealed a statistically significant, ~30% increase in the size ratios between *wild-type/wild-type* and *wild-type/Ptp61F^{Δ/Δ}* twin-clones in wing imaginal discs.

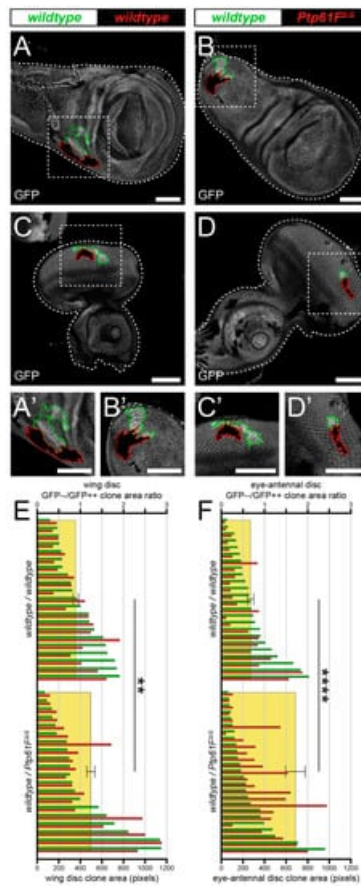


Figure 1. *Ptp61F* loss enhances epithelial clone relative fitness. **(A-D)** Confocal images of L3 imaginal tissues of the indicated genotypes (boxes at top, white indicates GFP-positive clones, black indicates remaining GFP-negative tissue) taken from animals where twin-clones were generated. The twins were either GFP-double positive (outlined in green) or GFP negative (outlined in red), with all other cells being GFP-single positive. **(A,B)** Twin clone analysis in wing imaginal discs. **(A,A')** In wing imaginal discs, the GFP-double-positive clones in *wild-type/wild-type* twins are slightly larger (twin-clone size ratio $\bar{x} = 0.895 \pm 0.091$). **(B,B')** The reverse is true for wing disc *wild-type/Ptp61F Δ/Δ* twin-clones, with the GFP-negative mutant clones being generally larger (twin-clone size ratio $\bar{x} = 1.244 \pm 0.093$). **(C-D)** Twin clone analysis in eye-antennal imaginal discs. **(C,C')** In eye-antennal imaginal discs, the GFP-double-positive clones in *wild-type/wild-type* twin-clones are again generally larger (twin-clone size ratio $\bar{x} = 0.680 \pm 0.072$). **(D,D')** Similarly, eye-antennal *wild-type/Ptp61F Δ/Δ* twin-clones have generally larger GFP-negative mutant clones (twin-clone size ratio $\bar{x} = 1.712 \pm 0.228$). **(E)** Quantification of L3 wing imaginal disc clone size profiles from *wild-type/wild-type* and *wild-type/Ptp61F Δ/Δ* twin-clone pairs. Green bars indicate the GFP-double-positive clone of the twin-clone pair, and red bars indicate the GFP-negative clone, and use the lower x-axis. Yellow rectangles indicate the average GFP-negative/GFP-double-positive clone area ratios, and use the upper x-axis, showing that *Ptp61F Δ/Δ* clones are significantly larger than the *wild-type* twin-clones (Student's *t*-test, d.f. = 39, $t = 3.169$, $p < 0.01$). **(F)** Quantification of L3 eye-antennal imaginal disc clone size profiles from *wild-type/wild-type* and *wild-type/Ptp61F Δ/Δ* twin-clone pairs. Green bars indicate the GFP-double-positive clone of the twin-clone pair, and red bars indicate the GFP-negative clone, and use the lower x-axis. Yellow rectangles indicate the average GFP-negative/GFP-double-positive clone area ratios, and use the upper x-axis, showing that *Ptp61F Δ/Δ* clones are significantly larger than the *wild-type* twin-clones (Student's *t*-test, d.f. = 47, $t = 4.272$, $p < 0.0001$). ** = $p < 0.01$, **** = $p < 0.0001$. Error bars = S.E.M. Note that clones were observed in all regions of both the eye-antennal and wing disc tissues, but that the figures show representative clones with GFP-negative/GFP-double-positive clone area ratios close to the average. Confocal microscopy images are single planes. Boxes in **(A-D)** are represented in **(A'-D')**, and dotted lines outline the tissue. Scale bars = 100 μ m.

These results are supported by similar findings in experiments using L3 eye-antennal imaginal discs, where *wild-type/wild-type* twins were observed to have a slightly larger GFP-double-positive twin (**Figure**

1C,C',F), but *wild-type/Ptp61F^{ΔΔ}* twins had a consistently larger GFP-negative, *Ptp61F* mutant twin (Figure 1D,D',F). Similar to the wing discs, the GFP-negative/GFP-double-positive size ratio was significantly larger in *wild-type/Ptp61F^{ΔΔ}* twins compared to *wild-type/wild-type* twins, by ~2-fold. Altogether, these data show that loss of *Ptp61F* confers a competitive advantage upon epithelial tissue clones, possibly by promoting cell survival and/or proliferation.

3. Ptp61F Regulates Polarity-Impaired Clone Survival/Growth during Cell Competition

One mode of cell competition in *Drosophila* occurs during the removal of polarity-impaired (such as *scrib* or *dlg1* mutant) cells from larval epithelial tissues, where these mutant cells are actively outcompeted and eliminated from epithelial tissue by mechanisms involving several cell competition and signalling pathways (reviewed in [16]). The twin-clone analyses suggested that PTP61F has a role in suppressing the ability of cells to compete, reducing their relative fitness and facilitating their elimination, as knocking-out *Ptp61F* clonally allows cells to outcompete their neighbours (Figure 1). The authors then tested whether *Ptp61F* reduction in cells that are relatively less fit (e.g., *scrib* mutant cells) might abrogate their elimination phenotype (Figure 2A). To investigate this, the mosaic analysis with a repressible cell marker (MARCM) technique was used, allowing for transgenes of interest and cell markers to be expressed in cells mutated for a gene-of-interest [51]. Using L3 eye-antennal imaginal discs, it was examined how *Ptp61F* knockdown affected the growth of clones with mutant *scrib* (*scrib^{1/1}*) that have a loser cell fate. In control discs, where both GFP-marked clones and the remainder of the tissue were otherwise *wild-type* (except that a *UAS-myr RFP* transgene was present in RNAi-free control samples as a *UAS* balancing element, and *UAS-Dcr-2* (a.k.a. Dicer) was also present in all samples), the induced clones make up ~40% of the tissue volume (Figure 2B,F). Expression of RNAi against *Ptp61F* (v37436) alone did not significantly alter this clonal tissue volume, with it remaining ~40% (Figure 2C,F). When clones homozygous for mutant *scrib* were induced, they contributed to a markedly smaller proportion of the total tissue volume, at ~11% (Figure 2D,F). However, expression of RNAi against *Ptp61F* within those *scrib^{1/1}* clones led to a small but statistically significant increase in their total volume to ~13% of the total tissue (Figure 2E,F). These data suggest that *Ptp61F* has a role, albeit small, in suppressing the ability of polarity-impaired cells to “fight back” against the efforts of neighbouring *wild-type* cells to eliminate them.

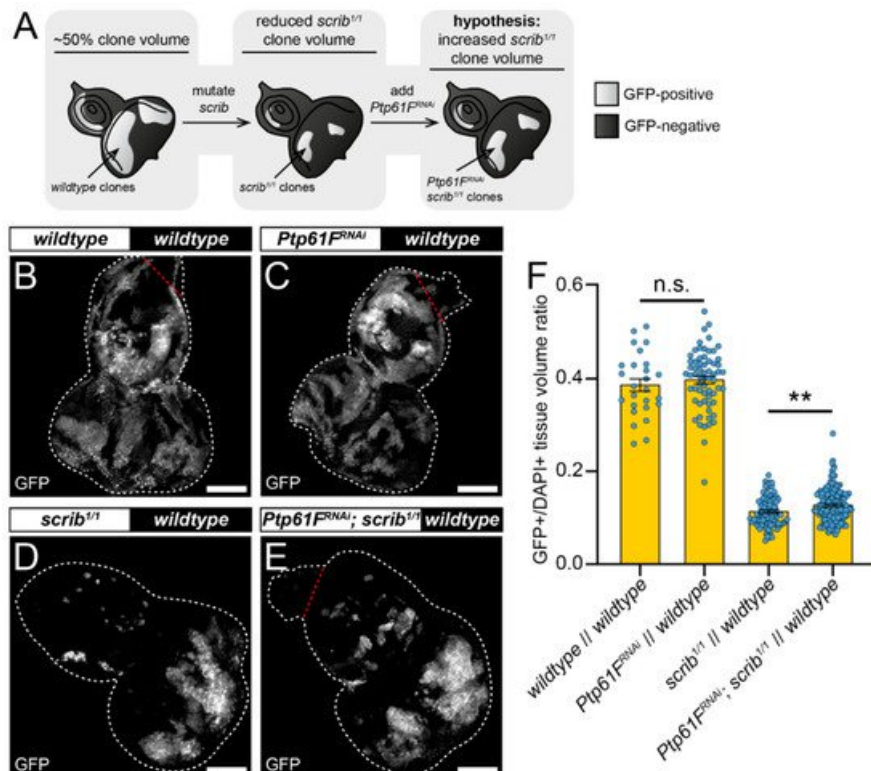


Figure 2. Ptp61F contributes to *scrib*-mutant clone elimination. **(A)** Diagram of our experimental process and hypothesis. **(B-E)** Confocal images of L3 eye-antennal imaginal discs of the indicated genotypes

(boxes at top, white indicates GFP-positive clones, black indicates remaining GFP-negative tissue) taken from animals where clones were generated via MARCM to express transgenes in *scrib*-mutant, GFP-positive cells. **(B,C)** When GFP-positive tissue is *wild-type* **(B)** it makes up ~40% of the tissue ($n = 26, \bar{x} = 0.386 \pm 0.013$), and *Ptp61F^{RNAi}* expression **(C)** does not significantly alter the contribution of the clones to the tissue ($n = 64, \bar{x} = 0.397 \pm 0.008$) (Student's *t*-test, d.f. = 88, $t = 0.7263, p > 0.05$). **(D,E)** *scrib*-mutant clones **(D)** make up only ~11% of the tissue ($n = 88, \bar{x} = 0.113 \pm 0.003$), but *Ptp61F^{RNAi}* expressed in *scrib*-mutant clones **(E)** leads to a small, but statistically significant increase in clonal volume to ~13% ($n = 144, \bar{x} = 0.127 \pm 0.003$) (Student's *t*-test, d.f. = 230, $t = 2.829, p < 0.01$). **(F)** Quantification of the clone tissue volume contributions, as measured by the ratio of GFP-positive tissue to DAPI-positive tissue, showing that *Ptp61F* knockdown significantly increases the size of *scrib*-mutant clones. Note that *Dcr-2* is also expressed wherever *GFP* is expressed. ** = $p < 0.01$. Error bars = S.E.M. Confocal microscopy images are maximum intensity projections. White dotted lines outline the tissue, red dotted lines indicate tissue excluded from quantification for consistency. Scale bars = 100 μ m.

4. JAK-STAT Signalling Plays a Role in the Fitness of Scrib-Mutant Clones and Is Required Downstream of Ptp61F Knockdown for the Increased Survival of Scrib-Mutant Clones

The data thus far have demonstrated a new role for PTP61F as contributing to polarity-impaired cell competition. Previous studies have shown that PTP61F can attenuate JAK-STAT signalling in *Drosophila* [24][25][26][27][52], but whether PTP61F regulates JAK-STAT signalling in the context of cell competition is unclear. Moreover, although JAK-STAT signalling is known to play a role in the *wild-type* winner cells during polarity-impaired cell competition [53], it is unclear whether JAK-STAT signalling has a role within the polarity-impaired loser cells. Therefore, using MARCM techniques, the authors investigated the requirement of JAK-STAT signalling in the competitiveness of polarity-impaired cells, and whether this occurs downstream of PTP61F.

RNAi against *Stat92E* (v43866) was used to determine whether JAK-STAT signalling is necessary for *scrib*-mutant clone elimination. Eye-antennal discs expressing *Stat92E^{RNAi}* had clones contributing to ~20% of the tissue volume, a significantly smaller fraction than the *wild-type* controls at ~40% (compare **Figure 3A,C**, quantified in **Figure 3I**), consistent with *Stat92E* influencing clonal fitness. Similarly, discs with *Stat92E^{RNAi}*-expressing *scrib^{1/1}* clones contributed to ~5% of the tissue volume, which was a significantly smaller proportion than the *scrib^{1/1}* controls at ~11% (compare **Figure 3E,G**, quantified in **Figure 3I**). These data suggest that STAT92E functions within *scrib*-mutant clones during cell competition to oppose their elimination.

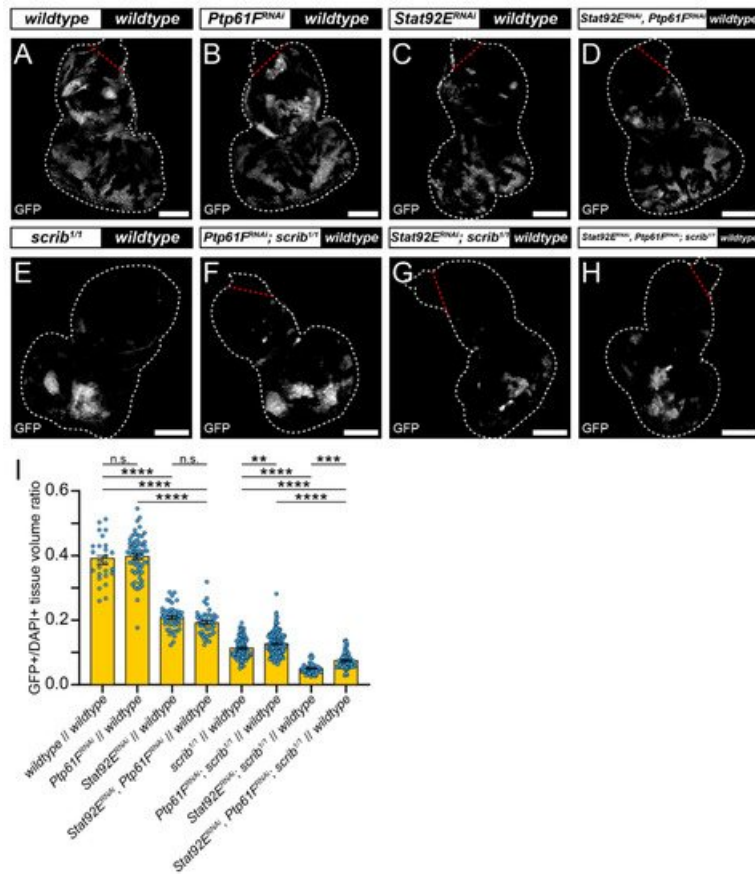


Figure 3. *Stat92E* is required for rescue of *scrib*-mutant clone size by *Ptp61F* knockdown. **(A-H)** Confocal images of L3 eye-antennal imaginal discs of the indicated genotypes (boxes at top, white indicates GFP-positive clones, black indicates remaining GFP-negative tissue) taken from animals where clones were generated via MARCM to express transgenes in GFP-positive cells. **(A-D)** *Wild-type* clones **(A)** and *Ptp61F^{RNAi}*-expressing **(B)** clones appear largely the same (for statistics see **Figure 2**). *Stat92E^{RNAi}* expression in a *wild-type* background (**(C)**; $n = 48$, $\bar{x} = 0.208 \pm 0.005$) leads to significantly smaller clones compared to the *wild-type* control (one-way ANOVA (**(F)** (3,175) = 193.3, $p < 0.0001$), with Tukey's multiple comparisons ($p < 0.0001$)), and combining *Stat92E* and *Ptp61F* knockdown in a *wild-type* background (**(D)**; $n = 41$, $\bar{x} = 0.192 \pm 0.006$) does not result in significantly different clone sizes to *Stat92E* knockdown alone (one-way ANOVA (**(F)** (3,175) = 193.3, $p > 0.05$), with Tukey's multiple comparisons ($p > 0.05$)), but does significantly reduce the average clone size relative to *Ptp61F^{RNAi}* clones (one-way ANOVA (**(F)** (3,175) = 193.3, $p > 0.05$), with Tukey's multiple comparisons ($p > 0.05$)). **(E-H)** Clones homozygous mutant for *scrib* **(E)** have their reduced volume somewhat rescued by *Ptp61F* knockdown **(F)** (for statistics see **Figure 2**). Knockdown of *Stat92E* in a *scrib*-mutant background (**(G)**; $n = 51$, $\bar{x} = 0.050 \pm 0.002$) leads to clones that are significantly smaller in their contribution to the tissue volume than the *scrib*-mutant control (one-way ANOVA (**(F)** (3,342) = 97.72, $p < 0.0001$), with Tukey's multiple comparisons ($p < 0.0001$)). Simultaneous knockdown of *Stat92E* and *Ptp61F* in *scrib^{1/1}* clones (**(H)**; $n = 63$, $\bar{x} = 0.075 \pm 0.003$) led to a statistically significant increase in clone volume relative to *scrib*-mutant, *Stat92E* knockdown clones (one-way ANOVA (**(F)** (3,342) = 97.72, $p < 0.0001$), with Tukey's multiple comparisons ($p < 0.001$)), and also resulted in a statistically significant decrease in clone volume compared to *scrib*-mutant, *Ptp61F^{RNAi}*-expressing clones (one-way ANOVA (**(F)** (3,342) = 97.72, $p < 0.0001$), with Tukey's multiple comparisons ($p < 0.0001$)). **(I)** Quantification of the clone tissue volume contributions, as measured by the ratio of GFP-positive tissue to DAPI-positive tissue, showing that simultaneous *Ptp61F* and *Stat92E* knockdown significantly increases the size of *scrib*-mutant clones compared to *Stat92E* knockdown alone in *scrib*-mutant clones. Note that some sample sets here are taken from **Figure 2**, as the experiments were performed under the same conditions and soon afterwards allowing them to be utilised as controls. Note that *Dcr-2* is also expressed wherever *GFP* is expressed. ** = $p < 0.01$, *** = $p < 0.001$, **** = $p < 0.0001$. Error bars = S.E.M. Confocal microscopy images are single planes. White dotted lines outline the tissue, red dotted lines indicate tissue excluded from

quantification for consistency. Scale bars = 100 μ m.

Next, it was examined whether elevated JAK-STAT signalling was driving *scrib*-mutant clone growth suppression upon *Ptp61F* knockdown. To analyse this *Stat92E* and *Ptp61F* were both knocked down in MARCM-generated clonal tissue. In otherwise *wild-type* clones, expression of both *Stat92E^{RNAi}* and *Ptp61F^{RNAi}* resulted in clones that contributed to ~20% of the tissue, a non-significant effect relative to the *Stat92E* knockdown alone (also ~20%; compare **Figure 3C,D**, quantified in **Figure 3I**). However, these clones were significantly smaller than the *Ptp61F^{RNAi}*-only clones (tissue volume of ~40%; compare **Figure 3B,D**, quantified in **Figure 3I**). By contrast, in *scrib*-mutant clones (which contribute to 11% of the tissue), simultaneous *Ptp61F* and *Stat92E* knockdown led to clones contributing to ~7% of the tissue, a statistically significant decrease in clonal tissue volume compared to *scrib*-mutant *Ptp61F* knockdown-only clones at ~13% (compare **Figure 3F,H**, quantified in **Figure 3I**), revealing a requirement for *Stat92E* in the *Ptp61F*-knockdown-mediated rescue of *scrib*-mutant clone size. In comparison with *scrib*-mutant *Stat92E* knockdown-only clones, which made up only ~5% of the tissue, simultaneous *Ptp61F* and *Stat92E* knockdown in *scrib*-mutant clones resulted in a statistically significant increase to 7% in clonal tissue volume (compare **Figure 3G,H**, quantified in **Figure 3I**), showing that the presence of *Ptp61F* contributes to the competitive disadvantage of *scrib*-mutant *Stat92E* knockdown clones. Together, these data show that STAT92E levels influence the survival of *scrib*-mutant clones, and that the increased survival of *scrib*-mutant clones upon *Ptp61F* knockdown is dependent on *Stat92E*.

References

1. Cheng, L.Y.; Parsons, L.M.; Richardson, H.E. Modelling Cancer in Drosophila: The Next Generation. In eLS; John Wiley & Sons, Ltd.: Chichester, UK, 2013.
2. Gonzalez, C. Drosophila melanogaster: A model and a tool to investigate malignancy and identify new therapeutics. Nat. Rev. Cancer 2013, 13, 172-183.
3. Sonoshita, M.; Cagan, R.L. Modeling Human Cancers in Drosophila. In Current Topics in Developmental Biology—Fly Models of Human Diseases; Pick, L., Ed.; Academic Press: Cambridge, MA, USA, 2017; pp. 287-309.
4. Richardson, H.E.; Portela, M. Modelling Cooperative Tumorigenesis in Drosophila. BioMed Res. Int. 2018, 2018, 4258387.
5. La Marca, J.E.; Richardson, H.E. Two-Faced: Roles of JNK Signalling During Tumorigenesis in the Drosophila Model. Front. Cell Dev. Biol. 2020, 8, 42.
6. Karim, F.D.; Rubin, G.M. Ectopic expression of activated Ras1 induces hyperplastic growth and increased cell death in Drosophila imaginal tissues. Development 1998, 125, 1-9.
7. Pagliarini, R.A.; Xu, T. A Genetic Screen in Drosophila for Metastatic Behavior. Science 2003, 302, 1227-1231.
8. Bilder, D.; Li, M.; Perrimon, N. Cooperative Regulation of Cell Polarity and Growth by Drosophila Tumor Suppressors. Science 2000, 289, 113-116.
9. Bilder, D.; Perrimon, N. Localization of apical epithelial determinants by the basolateral PDZ protein Scribble. Nature 2000, 403, 676-680.
10. Brumby, A.M.; Richardson, H.E. Scribble mutants cooperate with oncogenic Ras or Notch to cause neoplastic overgrowth in Drosophila. EMBO J. 2003, 22, 5769-5779.
11. Leong, G.R.; Goulding, K.R.; Amin, N.; Richardson, H.E.; Brumby, A.M. Scribble mutants promote aPKC and JNK-dependent epithelial neoplasia independently of Crumbs. BMC Biol. 2009, 7, 62.
12. Ma, X.; Xu, W.; Zhang, D.; Yang, Y.; Li, W.; Xue, L. Wallenda regulates JNK-mediated cell death in Drosophila. Cell Death Dis. 2015, 6, 1737.
13. Igaki, T.; Pagliarini, R.A.; Xu, T. Loss of Cell Polarity Drives Tumor Growth and Invasion through JNK Activation in Drosophila. Curr. Biol. 2006, 16, 1139-1146.
14. Uhlirva, M.; Jasper, H.; Bohmann, D. Non-cell-autonomous induction of tissue overgrowth by JNK/Ras cooperation in a Drosophila tumor model. Proc. Natl. Acad. Sci. USA 2005, 102, 13123-13128.
15. Chen, C.-L.; Schroeder, M.; Kango-Singh, M.; Tao, C.; Halder, G. Tumor suppression by cell competition through regulation of the Hippo pathway. Proc. Natl. Acad. Sci. USA 2012, 109, 484-489.
16. Fahey-Lozano, N.; La Marca, J.E.; Portela, M.; Richardson, H.E. Drosophila Models of Cell Polarity and Cell Competition in Tumorigenesis. In Advances in Experimental Medicine and Biology—The Drosophila Model in Cancer; Deng, W.-M., Ed.; Springer: Cham, Switzerland, 2019; pp. 36-74.
17. Madan, E.; Gogna, R.; Moreno, E. Cell competition in development: Information from flies and vertebrates. Curr. Opin. Cell Biol. 2018, 55, 150-157.

18. Cohen, P.T.W. Novel protein serine/threonine phosphatases: Variety is the spice of life. *Trends Biochem. Sci.* 1997, 22, 245–251.
19. Tonks, N.K. Protein tyrosine phosphatases—From housekeeping enzymes to master regulators of signal transduction. *FEBS J.* 2013, 280, 346–378.
20. Tonks, N.K. Protein tyrosine phosphatases: From genes, to function, to disease. *Nat. Rev. Mol. Cell Biol.* 2006, 7, 833–846.
21. Hatzihristidis, T.; Liu, S.; Pyszczyk, L.; Hutchins, A.P.; Gabaldon, T.; Tremblay, M.; Miranda-Saavedra, D. PTP-central: A comprehensive resource of protein tyrosine phosphatases in eukaryotic genomes. *Methods* 2014, 65, 156–164.
22. Morrison, D.K.; Murakami, M.S.; Cleghon, V. Protein Kinases and Phosphatases in the *Drosophila* Genome. *J. Cell Biol.* 2000, 150, 57–62.
23. Thurmond, J.; Goodman, J.L.; Strelets, V.B.; Attrill, H.; Gramates, L.S.; Marygold, S.J.; Matthews, B.B.; Millburn, G.; Antonazzo, G.; Trovisco, V.; et al. FlyBase 2.0: The next generation. *Nucleic Acids Res.* 2018, 47, 759–765.
24. Buszard, B.J.; Johnson, T.K.; Meng, T.-C.; Burke, R.; Warr, C.G.; Tiganis, T. The Nucleus- and Endoplasmic Reticulum-Targeted Forms of Protein Tyrosine Phosphatase 61F Regulate *Drosophila* Growth, Life Span, and Fecundity. *Mol. Cell Biol.* 2013, 33, 1345–1356.
25. Müller, P.; Kutteneuler, D.; Gesellchen, V.; Zeidler, M.P.; Boutros, M. Identification of JAK/STAT signalling components by genome-wide RNA interference. *Nature* 2005, 436, 871–875.
26. Saadin, A.; Starz-Gaiano, M. Identification of Novel Regulators of the JAK/STAT Signaling Pathway that Control Border Cell Migration in the *Drosophila* Ovary. *G3 Genes Genomes Genet.* 2016, 6, 1991–2002.
27. Willoughby, L.F.; Manent, J.; Allan, K.; Lee, H.; Portela, M.; Wiede, F.; Warr, C.; Meng, T.-Z.; Tiganis, T.; Richardson, H.E. Differential regulation of protein tyrosine kinase signalling by Dock and the PTP61F variants. *FEBS J.* 2017, 284, 2231–2250.
28. Tchankouo-Nguetcheu, S.; Udinotti, M.; Durand, M.; Meng, T.Z.; Taouis, M.; Rabinow, L. Negative regulation of MAP kinase signaling in *Drosophila* by Ptp61F/PTP1B. *Mol. Genet. Genom.* 2014, 289, 795–806.
29. Wu, C.-L.; Buszard, B.; Teng, C.H.; Chen, W.L.; Warr, C.G.; Tiganis, T.; Meng, T.C. Dock/Nck facilitates PTP61F/PTP1B regulation of insulin signalling. *Biochem. J.* 2011, 439, 151–159.
30. Hatzihristidis, T.; Desai, N.; Hutchins, A.P.; Meng, T.-C.; Tremblay, M.; Miranda-Saavedra, D. A *Drosophila*-centric view of protein tyrosine phosphatases. *FEBS Lett.* 2015, 589, 951–966.
31. Tiganis, T. PTP1B and TCPTP—Nonredundant phosphatases in insulin signaling and glucose homeostasis. *FEBS J.* 2013, 280, 445–458.
32. Tonks, N.K.; Diltz, C.D.; Fischer, E.H. Purification of the major protein-tyrosine-phosphatases of human placenta. *J. Biol. Chem.* 1988, 263, 6722–6730.
33. Elchebly, M. Increased Insulin Sensitivity and Obesity Resistance in Mice Lacking the Protein Tyrosine Phosphatase-1B Gene. *Science* 1999, 283, 1544–1548.
34. Galic, S.; Hauser, C.; Kahn, B.B.; Haj, F.G.; Neel, B.G.; Tonks, N.K.; Tiganis, T. Coordinated Regulation of Insulin Signaling by the Protein Tyrosine Phosphatases PTP1B and TCPTP. *Mol. Cell Biol.* 2005, 25, 819–829.
35. Klamann, L.D.; Boss, O.; Perroni, O.; Kim, J.K.; Martino, J.L.; Zabolotny, J.M.; Moghal, N.; Lubkin, M.; Kim, Y.B.; Sharpe, A.; et al. Increased Energy Expenditure, Decreased Adiposity, and Tissue-Specific Insulin Sensitivity in Protein-Tyrosine Phosphatase 1B-Deficient Mice. *Mol. Cell Biol.* 2000, 20, 5479–5489.
36. Myers, M.P. TYK2 and JAK2 are substrates of protein-tyrosine phosphatase 1B. *J. Biol. Chem.* 2001, 276, 47771–47774.
37. Zhu, S.; Bjorge, J.D.; Fujita, D.J. PTP1B Contributes to the Oncogenic Properties of Colon Cancer Cells through Src Activation. *Cancer Res.* 2007, 67, 10129–10137.
38. Arias-Romero, L.E.; Saha, S.; Villamar-Cruz, O.; Yip, S.C.; Ethier, S.P.; Zhang, Z.-Y.; Chernoff, J. Activation of Src by Protein Tyrosine Phosphatase 1B Is Required for ErbB2 Transformation of Human Breast Epithelial Cells. *Cancer Res.* 2009, 69, 4582–4588.
39. Bentires-Alj, M.; Neel, B.G. Protein-Tyrosine Phosphatase 1B Is Required for HER2/Neu-Induced Breast Cancer. *Cancer Res.* 2007, 67, 2420–2424.
40. Julien, S.G.; Dube, N.; Read, M.; Penney, J.; Paquet, M.; Han, Y.; Kennedy, B.P.; Muller, W.; Tremblay, M. Protein tyrosine phosphatase 1B deficiency or inhibition delays ErbB2-induced mammary tumorigenesis and protects from lung metastasis. *Nat. Genet.* 2007, 39, 338–346.
41. Lorenzen, J.A.; Dadabay, C.Y.; Fischer, E.H. COOH-terminal sequence motifs target the T cell protein tyrosine phosphatase to the ER and nucleus. *J. Cell Biol.* 1995, 131, 631–643.
42. Mosinger, B.; Tillmann, U.; Westphal, H.; Tremblay, M.L. Cloning and characterization of a mouse cDNA encoding a cytoplasmic protein-tyrosine-phosphatase. *Proc. Natl. Acad. Sci. USA* 1992, 89, 499–503.
43. Tiganis, T.; Flint, A.J.; Adam, S.A.; Tonks, N.K. Association of the T-cell Protein Tyrosine Phosphatase with Nuclear Import Factor p97. *J. Biol. Chem.* 1997, 272, 21548–21557.
44. Tiganis, T.; Bennett, A.M. Protein tyrosine phosphatase function: The substrate perspective. *Biochem. J.* 2007, 402, 1–15.
45. Kleppe, M.; Lahortiga, I.; El Chaar, T.; De Keersmaecker, K.; Mentens, N.; Graux, C.; Van Roosbroeck, K.; Ferrardo, A.A.;

- Langerak, A.; Meijerink, J.P.P.; et al. Deletion of the protein tyrosine phosphatase gene PTPN2 in T-cell acute lymphoblastic leukemia. *Nat. Genet.* 2010, 42, 530-535.
46. Kleppe, M.; Soulier, J.; Asnafi, V.; Mentens, N.; Hornakova, T.; Knoops, L.; Constantinescu, S.; Sigaux, F.; Meijerink, J.P.; Vandenberghe, P.; et al. PTPN2 negatively regulates oncogenic JAK1 in T-cell acute lymphoblastic leukemia. *Blood* 2011, 117, 7090-7098.
47. Shields, B.J.; Wiede, F.; Gurzov, E.N.; Wee, K.; Hauser, C.; Zhu, H.-J.; Molloy, T.J.; O'Toole, S.A.; Daly, R.; Sutherland, R.L.; et al. TCPTP Regulates SFK and STAT3 Signaling and Is Lost in Triple-Negative Breast Cancers. *Mol. Cell. Biol.* 2013, 33, 557-570.
48. Tiganis, T. The Role of TCPTP in Cancer. In *Protein Tyrosine Phosphatases in Cancer*; Neel, B.G., Tonks, N.K., Eds.; Springer: New York, NY, USA, 2016; pp. 145-168.
49. Grohmann, M.; Wiede, F.; Dodd, G.; Gurzov, E.N.; Ooi, G.; Butt, T.; Rasmiena, A.A.; Kaur, S.; Gulati, T.; Goh, P.K.; et al. Obesity Drives STAT-1-Dependent NASH and STAT-3-Dependent HCC. *Cell* 2018, 175, 1289-1306.
50. Foldi, F.; Ziosi, M.; Garoia, F.; Pession, A.; Grzeschik, N.A.; Bellosta, P.; Strand, D.; Richardson, H.E.; Pession, A.; Griffoni, D. The lethal giant larvae tumour suppressor mutation requires dMyc oncoprotein to promote clonal malignancy. *BMC Biol.* 2010, 8, 33.
51. Lee, T.; Luo, L. Mosaic Analysis with a Repressible Cell Marker for Studies of Gene Function in Neuronal Morphogenesis. *Neuron* 1999, 22, 451-461.
52. Baeg, G.-H.; Zhou, R.; Perrimon, N. Genome-wide RNAi analysis of JAK/STAT signaling components in *Drosophila*. *Genes Dev.* 2005, 19, 1861-1870.
53. Schroeder, M.C.; Chen, C.-L.; Gajewski, K.; Halder, G. A non-cell-autonomous tumor suppressor role for Stat in eliminating oncogenic scribble cells. *Oncogene* 2013, 32, 4471-4479.

Keywords

PTP61F;RAS;JAK-STAT;cell competition

Retrieved from <https://encyclopedia.pub/17813>